

Surface Resistance and Amplitude Mode under Uniform and Static External Field in Conventional Superconductors

Takanobu Jujo*

*Division of Materials Science, Graduate School of Science and Technology, Nara
Institute of Science and Technology, Ikoma, Nara 630-0101, Japan*

We calculate the surface resistance of s-wave superconductors under a static external field on the basis of the quasiclassical approximation. The numerical calculations are performed both for the dirty and relatively clean cases, and the difference in the absorption spectrum between them is investigated. The amplitude mode in the dirty case, which has been previously studied in the local response function, appears also in the nonlocal response. In the clean case, there is a large discrepancy between the excitation energy of the amplitude mode and the energy of the gap edge where the coupling between the electrons and the external field is effective. Therefore, the amplitude mode exists even when the superconductor is relatively clean, but its contribution to the response function is small. These behaviors, which are qualitatively consistent with the experimental results, are obtained by taking into account the static field nonperturbatively.

1. Introduction

In recent years, the observation of nonequilibrium states in the superconducting state has progressed owing to the advancement of the microwave spectroscopy in experiments.¹⁾ The excitation and relaxation of quasiparticles and collective modes have been observed by pump-probe spectroscopy.^{2,3)} As a major development, the amplitude mode, which was difficult to observe because it did not appear in the linear response, has been discussed in the nonlinear response with experimental⁴⁻⁷⁾ and theoretical methods.⁸⁻¹²⁾

On the other hand, the generation of nonequilibrium states is possible not only by optical excitation but also by stationary fields (magnetic field and current), which has been studied for a long time. For example, one-particle properties such as the density of states have been investigated experimentally^{13,14)} and theoretically.¹⁵⁾ A similarity

*E-mail address: jujo@ms.aist-nara.ac.jp

of the one-particle spectrum between dirty superconductors under a static field and those including paramagnetic impurities was discussed.¹⁶⁾ Collective modes are included in the one-particle state through self-energy,¹⁷⁾ but these characteristics are obscured through integrations by the energy and wave numbers. On the other hand, since in the response function collective modes can emerge through the final state interaction (vertex corrections), it is possible that these characteristics appear more directly.

The response function in the nonequilibrium state under a static field has also been studied theoretically,^{18–22)} but there remain several properties to be investigated as compared with the case of the one-particle state. For example, in the surface resistance, the existence (absence) of a peak structure around the gap edge has been experimentally observed for dirty (clean) superconductors.^{23,24)} A theoretical proposal with a surface state has been made to solve this problem,^{25,26)} but its relevance to the response function is not obvious. The perturbative calculation with static fields suggested a relationship between the peak structure in the response function and the collective mode.^{22,27)} (The peak has also been observed recently in an experiment in dirty *s*-wave superconductors.²⁸⁾) However, the perturbative calculation cannot explain the absorption edge and the absence of the peak in the clean case.

The gap edge of the density of states under a static field is not determined by the superconducting order parameter irrespective of whether the superconductor is dirty or clean. Therefore, in order to calculate the surface resistance, it is necessary to take into account the static field nonperturbatively. In this paper, we consider this problem and calculate the nonlocal response function under a static field to derive the surface resistance in both dirty and relatively clean superconductors. So far, the amplitude mode has been discussed on the basis of the local response function. In this study, we show that the amplitude mode can appear even when nonlocality is important, and we clarify the reason why the amplitude mode is not visible in the absorption spectrum in the case of relatively clean superconductors.

The structure of this paper is as follows. Section 2 shows how to calculate the surface impedance using the quasiclassical approximation. This calculation derives vertex correction terms due to impurity scattering and electron–phonon interaction. The latter includes the amplitude mode. Section 3 shows the results of the numerical calculation of the surface resistance, and the relationship between the one-particle spectrum and the response function is discussed. In Sect. 4, the relationship between the calculated and experimental results is discussed. We put $\hbar = c = 1$ in this paper (c is the velocity

of light).

2. Formulation

The surface impedance at the frequency ω is given by²⁹⁾

$$Z_S = \frac{4\pi E_\omega^x(z=0)}{H_\omega^y(z=0)}. \quad (1)$$

We consider the Cartesian coordinate system (x, y, z) . The external field is in the xy -plane, and there is an interface at $z = 0$ between the superconductor ($z > 0$) and the vacuum ($z < 0$). The electric field $E_\omega^x(z)$ [the magnetic field $H_\omega^y(z)$], which is parallel to the x (y) -axis and penetrates into $z > 0$ in the superconductor, is determined by the Maxwell equation

$$\frac{dE_\omega^x(z)}{dz} = i\omega H_\omega^y(z) \quad \text{and} \quad -\frac{dH_\omega^y(z)}{dz} = 4\pi j_\omega^x(z). \quad (2)$$

$j_\omega^x(z)$ is the current. (The displacement current term is omitted because of its smallness as mentioned in Sect. 3.) Using the Fourier transformation with the specular boundary condition³⁰⁾ [$E_\omega^x(z) = E_\omega^x(-z)$ and $j_\omega^x(z) = j_\omega^x(-z)$] : $\tilde{E}_\omega^x(q) = \int dz e^{-iqz} E_\omega^x(z)$ and $\tilde{j}_\omega^x(q) = \int dz e^{-iqz} j_\omega^x(z)$, Eq. (2) is written as

$$-q^2 \tilde{E}_\omega^x(q) = 2E_\omega^{x'}(z=0) - 4\pi i\omega \tilde{j}_\omega^x(q) \quad (3)$$

with $E_\omega^{x'}(z=0) = dE_\omega^x(z)/dz|_{z=0} = 4\pi i\omega \int_0^\infty j_\omega^x(z) dz$. Then, the surface impedance is rewritten as

$$Z_S = \frac{4\pi i\omega E_\omega^x(0)}{E_\omega^{x'}(0)} = 4\pi i\omega \int \frac{dq}{2\pi} \frac{-2}{q^2 - 4\pi i\tilde{j}_\omega^x(q)/\tilde{E}_\omega^x(q)}. \quad (4)$$

The current $j_\omega^x(z)$ is given by using the nonequilibrium quasiclassical Green function as³¹⁾

$$j_\omega^x(z) = e \int_{FS} v_{\mathbf{k}}^x \frac{mk_F}{2\pi} \int \frac{d\epsilon}{4\pi i} Tr [T_{\epsilon^-}^h \hat{g}_{\mathbf{k},\epsilon^+,\epsilon^-}^{+'}(z) - T_{\epsilon^+}^h \hat{g}_{\mathbf{k},\epsilon^+,\epsilon^-}^{-'}(z) + \hat{g}_{\mathbf{k},\epsilon^+,\epsilon^-}^{(a)'}(z)]. \quad (5)$$

Here, m and k_F are the mass of quasiparticles and the Fermi wave number, respectively. $v_{\mathbf{k}}^x$ is the quasiparticle velocity parallel to the x -axis [$\mathbf{v}_{\mathbf{k}} = (v_{\mathbf{k}}^x, v_{\mathbf{k}}^y, v_{\mathbf{k}}^z)$] at the Fermi surface ($|\mathbf{k}| = k_F$ and $|\mathbf{v}_{\mathbf{k}}| = v_F$). $\epsilon^\pm = \epsilon \pm \omega/2$ and $T_\epsilon^h := \tanh(\epsilon/2T)$ (T is the temperature). \int_{FS} and Tr mean the integration over the Fermi surface and taking the trace of the matrix, respectively. The nonequilibrium quasiclassical Green function [$\hat{g}_{\mathbf{k},\epsilon^+,\epsilon^-}^{\pm'}$ and $\hat{g}_{\mathbf{k},\epsilon^+,\epsilon^-}^{(a)'}$] under a uniform and static external field (represented by a vector potential \mathbf{A}_0) with the first order of $A_\omega^x(z) = E_\omega^x(z)/i\omega$ satisfies the following

equations:³¹⁾

$$\begin{aligned} \hat{\tau}_3 \left[\epsilon^+ \hat{1} + e\mathbf{v}_\mathbf{k} \cdot \mathbf{A}_0 \hat{1} - \hat{\Sigma}_{\epsilon^+}^+ \right] \hat{g}_{\mathbf{k},\epsilon^+,\epsilon^-}^{(a)'}(z) - \hat{g}_{\mathbf{k},\epsilon^+,\epsilon^-}^{(a)'}(z) \left[\epsilon^- \hat{1} + e\mathbf{v}_\mathbf{k} \cdot \mathbf{A}_0 \hat{1} - \hat{\Sigma}_{\epsilon^-}^- \right] \hat{\tau}_3 + iv_\mathbf{k}^z \frac{d\hat{g}_{\mathbf{k},\epsilon^+,\epsilon^-}^{(a)'}(z)}{dz} \\ - \hat{\tau}_3 \hat{\Sigma}_{\epsilon^+,\epsilon^-}^{(a)'}(z) \hat{g}_{\mathbf{k},\epsilon^-}^- + \hat{g}_{\mathbf{k},\epsilon^+}^+ \hat{\Sigma}_{\epsilon^+,\epsilon^-}^{(a)'}(z) \hat{\tau}_3 - (T_{\epsilon^+}^h - T_{\epsilon^-}^h) ev_\mathbf{k}^x A_\omega^x(z) \left(\hat{g}_{\mathbf{k},\epsilon^+}^+ \hat{\tau}_3 - \hat{\tau}_3 \hat{g}_{\mathbf{k},\epsilon^-}^- \right) = 0 \end{aligned} \quad (6)$$

and

$$\begin{aligned} \hat{\tau}_3 \left[\epsilon^+ \hat{1} + e\mathbf{v}_\mathbf{k} \cdot \mathbf{A}_0 \hat{1} - \hat{\Sigma}_{\epsilon^+}^+ \right] \hat{g}_{\mathbf{k},\epsilon^+,\epsilon^-}^{+'}(z) - \hat{g}_{\mathbf{k},\epsilon^+,\epsilon^-}^{+'}(z) \left[\epsilon^- \hat{1} + e\mathbf{v}_\mathbf{k} \cdot \mathbf{A}_0 \hat{1} - \hat{\Sigma}_{\epsilon^-}^- \right] \hat{\tau}_3 + iv_\mathbf{k}^z \frac{d\hat{g}_{\mathbf{k},\epsilon^+,\epsilon^-}^{+'}(z)}{dz} \\ - \hat{\tau}_3 \hat{\Sigma}_{\epsilon^+,\epsilon^-}^{+'}(z) \hat{g}_{\mathbf{k},\epsilon^-}^- + \hat{g}_{\mathbf{k},\epsilon^+}^+ \hat{\Sigma}_{\epsilon^+,\epsilon^-}^{+'}(z) \hat{\tau}_3 - ev_\mathbf{k}^x A_\omega^x(z) \left(\hat{g}_{\mathbf{k},\epsilon^+}^+ \hat{\tau}_3 - \hat{\tau}_3 \hat{g}_{\mathbf{k},\epsilon^-}^- \right) = 0, \end{aligned} \quad (7)$$

where $\hat{1} = \begin{pmatrix} 1 & 0 \\ 0 & 1 \end{pmatrix}$ and $\hat{\tau}_3 = \begin{pmatrix} 1 & 0 \\ 0 & -1 \end{pmatrix}$. $\hat{g}_{\mathbf{k},\epsilon}^\pm$ and $\hat{\Sigma}_\epsilon^\pm$ are the one-particle Green function and self-energy under the uniform and static field, respectively [+ (−) corresponds to the retarded (advanced) function]. $\hat{g}_{\mathbf{k},\epsilon}^\pm$ depends on the direction of Fermi wave number \mathbf{k} because of the term $e\mathbf{v}_\mathbf{k} \cdot \mathbf{A}_0$. $\hat{\Sigma}_{\epsilon^+,\epsilon^-}^{\pm'}$ and $\hat{\Sigma}_{\epsilon^+,\epsilon^-}^{(a)'}$ are the self-energies in the nonequilibrium state, which include the effect of $E_\omega^x(z)$ in the first order. We consider the electron–phonon interaction within the weak-coupling approximation³²⁾ and the impurity scattering with Born approximation. Then, the self-energy is written as

$$\hat{\Sigma}_\epsilon^\pm = \Delta \hat{\tau}_1 + \alpha \int_{FS} \hat{\tau}_3 \hat{g}_{\mathbf{k},\epsilon}^\pm \hat{\tau}_3. \quad (8)$$

Here, $\hat{\tau}_1 = \begin{pmatrix} 0 & 1 \\ 1 & 0 \end{pmatrix}$ and $\alpha := (mk_F/2\pi)n_i u_i^2$, where n_i and u_i are the concentration and potential of nonmagnetic impurities, respectively. [$\hat{g}_{\mathbf{k},\epsilon}^\pm$ is given in Eq. (13).] The superconducting gap Δ is determined by the gap equation

$$\Delta = p \int \frac{d\epsilon}{2\pi i} T_\epsilon^h \int_{FS} \frac{-1}{2} Tr[\hat{\tau}_1(\hat{g}_{\mathbf{k},\epsilon}^+ - \hat{g}_{\mathbf{k},\epsilon}^-)]. \quad (9)$$

Here, $p := (mk_F/2\pi)(g_{ph}^2/\omega_D)$, where g_{ph} is the electron-phonon coupling constant and ω_D the Debye frequency. Corresponding to this approximation, the self-energy in the nonequilibrium state is given by $\hat{\Sigma}_{\epsilon^+,\epsilon^-}^{\pm'}(z) = \hat{\Sigma}_\omega^{(ep)}(z) + \hat{\Sigma}_{\epsilon^+,\epsilon^-}^{\pm(im)}(z)$ with

$$\hat{\Sigma}_\omega^{(ep)}(z) = p \int \frac{d\epsilon}{2\pi i} \int_{FS} \hat{\tau}_3 \left[T_{\epsilon^-}^h \hat{g}_{\mathbf{k},\epsilon^+,\epsilon^-}^{+'}(z) - T_{\epsilon^+}^h \hat{g}_{\mathbf{k},\epsilon^+,\epsilon^-}^{-'}(z) + \hat{g}_{\mathbf{k},\epsilon^+,\epsilon^-}^{(a)'}(z) \right] \hat{\tau}_3 \quad (10)$$

and

$$\hat{\Sigma}_{\epsilon,\epsilon'}^{\pm(im)}(z) = \alpha \int_{FS} \hat{\tau}_3 \hat{g}_{\mathbf{k},\epsilon,\epsilon'}^{\pm'}(z) \hat{\tau}_3. \quad (11)$$

$$\hat{\Sigma}_{\epsilon^+,\epsilon^-}^{(a)' }(\mathbf{r}) = (T_{\epsilon^+}^h - T_{\epsilon^-}^h) \hat{\Sigma}_\omega^{(ep)}(z) + \alpha \int_{FS} \hat{\tau}_3 \hat{g}_{\mathbf{k},\epsilon^+,\epsilon^-}^{(a)' }(\mathbf{r}) \hat{\tau}_3. \quad (12)$$

[In the weak-coupling approximation, the diagonal term of $\hat{\Sigma}_\omega^{(ep)}(z)$ vanishes because of the relation $\hat{g}_{\mathbf{k},\epsilon^\pm}^+ \leftrightarrow -\hat{\tau}_3 \hat{g}_{\mathbf{k},\epsilon^\mp}^- \hat{\tau}_3$ under $\epsilon \leftrightarrow -\epsilon$ and $\mathbf{k} \leftrightarrow -\mathbf{k}$ in the integration of Eq. (10), and only the off-diagonal term remains in $\hat{\Sigma}_\omega^{(ep)}(z)$.] The one-particle Green function under the uniform and static field is given by

$$\hat{g}_{\mathbf{k},\epsilon}^\pm = -\frac{\tilde{\epsilon}_{\mathbf{k}}^\pm \hat{1} + \tilde{\Delta}_\epsilon^\pm \hat{\tau}_1}{\sqrt{(\tilde{\Delta}_\epsilon^\pm)^2 - (\tilde{\epsilon}_{\mathbf{k}}^\pm)^2}}. \quad (13)$$

Here, $\tilde{\epsilon}_{\mathbf{k}}^\pm = \epsilon + e\mathbf{v}_{\mathbf{k}} \cdot \mathbf{A}_0 - \Sigma_n^\pm(\epsilon)$ and $\tilde{\Delta}_\epsilon^\pm = \Sigma_a^\pm(\epsilon)$, in which $\Sigma_n^\pm(\epsilon)\hat{1} + \Sigma_a^\pm(\epsilon)\hat{\tau}_1 = \hat{\Sigma}_\epsilon^\pm$ [Eq. (8)]. We take the effect of $e\mathbf{v}_{\mathbf{k}} \cdot \mathbf{A}_0$ into account nonperturbatively in the calculation of the conductivity.

2.1 Vertex corrections

We solve Eqs. (7) and (6), and the current [the Fourier transform of Eq. (5)] is given by

$$\tilde{j}_\omega^x(q) = \tilde{j}_\omega^{x(0)}(q) + \tilde{j}_\omega^{x(im)}(q) + \tilde{j}_\omega^{x(ep)}(q), \quad (14)$$

in which $\tilde{j}_\omega^{x(0)}(q)$, $\tilde{j}_\omega^{x(im)}(q)$, and $\tilde{j}_\omega^{x(ep)}(q)$ indicate the term with no vertex corrections, the vertex correction term by impurity scattering, and the amplitude fluctuation mode term, respectively. These are written as

$$\tilde{j}_\omega^{x(x)}(q) = \frac{-3}{8\lambda_0^2} \int \frac{d\epsilon}{2\pi i} \left[T_{\epsilon^-, \epsilon^+}^h \kappa_{\epsilon^+, \epsilon^-}^{(x)++}(q) - T_{\epsilon^+, \epsilon^-}^h \kappa_{\epsilon^+, \epsilon^-}^{(x)--}(q) + (T_{\epsilon^+}^h - T_{\epsilon^-}^h) \kappa_{\epsilon^+, \epsilon^-}^{(x)+-}(q) \right] \tilde{A}_\omega^x(q) \quad (15)$$

with $x = 0, im, \text{ and } ep$. (λ_0 is the magnetic field penetration depth and $1/\lambda_0^2 = 4\pi e^2 n_e/m$ with the electron density $n_e = k_F^3/3\pi^2$.) $\kappa_{\epsilon^+, \epsilon^-}^{(0)ss'}$ (q), $\kappa_{\epsilon^+, \epsilon^-}^{(im)ss'}$ (q), and $\kappa_{\epsilon^+, \epsilon^-}^{(ep)ss'}$ (q) are given by

$$\kappa_{\epsilon^+, \epsilon^-}^{(0)ss'}(q) = \int_{FS} \left(\frac{v_{\mathbf{k}}^x}{v_F} \right)^2 \frac{(\zeta_{\mathbf{k},\epsilon^+}^s + \zeta_{\mathbf{k},\epsilon^-}^{s'})(1 + g_{\mathbf{k},\epsilon^+}^s g_{\mathbf{k},\epsilon^-}^{s'} + f_{\mathbf{k},\epsilon^+}^s f_{\mathbf{k},\epsilon^-}^{s'})}{(v_{\mathbf{k}}^z q)^2 + (\zeta_{\mathbf{k},\epsilon^+}^s + \zeta_{\mathbf{k},\epsilon^-}^{s'})^2} \quad (16)$$

($s, s' = \pm$), $\zeta_{\mathbf{k},\epsilon}^\pm = \sqrt{(\tilde{\Delta}_\epsilon^\pm)^2 - (\tilde{\epsilon}_{\mathbf{k}}^\pm)^2}$, and $g_{\mathbf{k},\epsilon}^\pm \hat{1} + f_{\mathbf{k},\epsilon}^\pm \hat{\tau}_1 = \hat{g}_{\mathbf{k},\epsilon}^\pm$.

$$\kappa_{\epsilon^+, \epsilon^-}^{(im)ss'}(q) = \frac{\alpha[\chi_1'^2 - \chi_3'^2 + \alpha(\chi_1'^2 \chi_2 - 2\chi_1' \chi_3' \chi_3 + \chi_1 \chi_3'^2)]}{(1 - \alpha\chi_1)(1 + \alpha\chi_2) + (\alpha\chi_3)^2} \quad (17)$$

and

$$\kappa_{\epsilon^+, \epsilon^-}^{(ep)ss'}(q) = 2\tilde{\Sigma}_a(\omega, q) \kappa_{\epsilon^+, \epsilon^-}^{ss'(v1)}(q) \quad (18)$$

with

$$\kappa_{\epsilon^+, \epsilon^-}^{ss'(v1)}(q) = \frac{\chi_3' + \alpha(\chi_1' \chi_3 - \chi_1 \chi_3')}{(1 - \alpha\chi_1)(1 + \alpha\chi_2) + (\alpha\chi_3)^2}, \quad (19)$$

$$\tilde{\Sigma}_a(\omega, q) = \frac{-(p/2) \int \frac{d\epsilon}{2\pi i} \left[T_{\epsilon^-}^h \kappa_{\epsilon^+, \epsilon^-}^{++(v1)}(q) - T_{\epsilon^+}^h \kappa_{\epsilon^+, \epsilon^-}^{--(v1)}(q) + (T_{\epsilon^+}^h - T_{\epsilon^-}^h) \kappa_{\epsilon^+, \epsilon^-}^{+- (v1)}(q) \right]}{1 + p \int \frac{d\epsilon}{2\pi i} \left[T_{\epsilon^-}^h \kappa_{\epsilon^+, \epsilon^-}^{++(v0)}(q) - T_{\epsilon^+}^h \kappa_{\epsilon^+, \epsilon^-}^{--(v0)}(q) + (T_{\epsilon^+}^h - T_{\epsilon^-}^h) \kappa_{\epsilon^+, \epsilon^-}^{+- (v0)}(q) \right]}, \quad (20)$$

and

$$\kappa_{\epsilon^+, \epsilon^-}^{ss'(v0)}(q) = \frac{\chi_2 + \alpha(\chi_3^2 - \chi_1\chi_2)}{(1 - \alpha\chi_1)(1 + \alpha\chi_2) + (\alpha\chi_3)^2}. \quad (21)$$

Here,

$$\begin{pmatrix} \chi'_1 \\ \chi'_3 \\ \chi'_2 \end{pmatrix} = \int_{FS} \frac{(v_{\mathbf{k}}^x/v_F)(\zeta_{\mathbf{k}, \epsilon^+}^s + \zeta_{\mathbf{k}, \epsilon^-}^{s'})}{(v_{\mathbf{k}}^z q)^2 + (\zeta_{\mathbf{k}, \epsilon^+}^s + \zeta_{\mathbf{k}, \epsilon^-}^{s'})^2} \begin{pmatrix} 1 + g_{\mathbf{k}, \epsilon^+}^s g_{\mathbf{k}, \epsilon^-}^{s'} + f_{\mathbf{k}, \epsilon^+}^s f_{\mathbf{k}, \epsilon^-}^{s'} \\ g_{\mathbf{k}, \epsilon^+}^s f_{\mathbf{k}, \epsilon^-}^{s'} + f_{\mathbf{k}, \epsilon^+}^s g_{\mathbf{k}, \epsilon^-}^{s'} \\ -1 + g_{\mathbf{k}, \epsilon^+}^s g_{\mathbf{k}, \epsilon^-}^{s'} + f_{\mathbf{k}, \epsilon^+}^s f_{\mathbf{k}, \epsilon^-}^{s'} \end{pmatrix}, \quad (22)$$

and $\chi_{1,2,3}$ are defined by similar relations with $(v_{\mathbf{k}}^x/v_F)$ replaced by 1 in Eq. (22). $\tilde{\Sigma}_a(\omega, q)$ is related to the off-diagonal part of the Fourier transform of Eq. (10) as

$$\tilde{\Sigma}_a(\omega, q) = \frac{-1}{2ev_F \tilde{A}_\omega^x(q)} Tr \left[\frac{1}{2} \hat{\tau}_1 \tilde{\Sigma}_\omega^{(ep)}(q) \right]. \quad (23)$$

The vertex correction terms take different values depending on the direction of \mathbf{A}_0 . The integrand of $\chi'_{1,2,3}$ is proportional to $v_{\mathbf{k}}^x$. When \mathbf{A}_0 is parallel to A_ω^x ($e\mathbf{v}_{\mathbf{k}} \cdot \mathbf{A}_0 = ev_{\mathbf{k}}^x A_0$), $\chi'_{1,2,3} \neq 0$ and the vertex correction terms take finite values. On the other hand, when \mathbf{A}_0 is perpendicular to A_ω^x ($e\mathbf{v}_{\mathbf{k}} \cdot \mathbf{A}_0 = ev_{\mathbf{k}}^y A_0$), $\chi'_{1,2,3} = 0$ ($\chi_{1,2,3} \neq 0$) and then the vertex correction terms vanish. We can consider the calculated results of the term with no vertex correction in Sect. 3 as the conductivity in the case that \mathbf{A}_0 is perpendicular to A_ω^x .

2.2 Absorption below $\omega < 2\Delta$

In this subsection, we show that there is a finite absorption below $\omega < 2\Delta$ even if $\alpha \ll \Delta$ when the self-energy correction is taken into account. For example, the real part of the optical conductivity with no vertex correction is written as

$$\text{Re} \left(\frac{\tilde{j}_\omega^{x(0)}(q)}{\tilde{E}_\omega^x(q)} \right) = \frac{3}{2\pi\omega\lambda_0^2} \int_0^{\omega/2} d\epsilon \text{Re} \left[\kappa_{\epsilon^+, \epsilon^-}^{(0)+-}(q) - \kappa_{\epsilon^+, \epsilon^-}^{(0)++}(q) \right] \quad (24)$$

for $T = 0$ and $\omega > 0$. $\kappa_{\epsilon^+, \epsilon^-}^{(0)ss'}(q)$ is given in Eq. (16). In the limit of small α , $\zeta_{\mathbf{k}, \epsilon}^\pm$ is given by

$$\zeta_{\mathbf{k}, \epsilon}^\pm \simeq \zeta_{\mathbf{k}, \epsilon}^{\prime\pm} + \alpha \zeta_{\mathbf{k}, \epsilon}^{\prime\pm} \int_{FS} (1/\zeta_{\mathbf{k}, \epsilon}^{\prime\pm}) \quad (25)$$

with

$$\zeta_{\mathbf{k}, \epsilon}^{\prime\pm} = \sqrt{\Delta^2 - (\epsilon'_k)^2} \theta(\Delta - |\epsilon'_k|) - i \text{sgn}(\pm \epsilon'_k) \sqrt{(\epsilon'_k)^2 - \Delta^2} \theta(|\epsilon'_k| - \Delta), \quad (26)$$

where $\epsilon'_k = \epsilon + e\mathbf{v}_k \cdot \mathbf{A}_0$ and $\theta(\cdot)$ is a step function. The imaginary part of the $\alpha\zeta'_{k,\epsilon} \int_{FS} (1/\zeta'_{k,\epsilon})$ term in Eq. (25) is finite for $|\epsilon| \geq \Delta - ev_F A_0$ in the clean case ($\alpha \ll \Delta$). This is because the term $e\mathbf{v}_k \cdot \mathbf{A}_0$ is included in the integration over the Fermi surface for the self-energy. Then, $\text{Re}[\cdot]$ in Eq. (24) takes finite values only in the case of $\epsilon + e\mathbf{v}_k \cdot \mathbf{A}_0 + \omega/2 > \Delta - ev_F A_0$ and $\epsilon + e\mathbf{v}_k \cdot \mathbf{A}_0 - \omega/2 < -\Delta + ev_F A_0$. This results in the finite absorption for $\omega > 2(\Delta - ev_F A_0)$ with a small but finite impurity scattering ($\alpha \neq 0$). If we mistakenly adopt an approximation $\alpha\zeta'_{k,\epsilon} \int_{FS} (1/\zeta'_{k,\epsilon}) \simeq \alpha$ in Eq. (25) by neglecting the self-energy effect, there is no absorption below $\omega < 2\Delta$ at $T = 0$ irrespective of the value of $\alpha > 0$. This approximation results in the absorption edge at $\omega = 2\Delta$.

3. Results of Numerical Calculations

We numerically calculate the surface impedance using Eqs. (4) and (14). We take Δ_0 (the superconducting gap in the case of $e\mathbf{v}_k \cdot \mathbf{A}_0 = 0$ and $T = 0$) as the unit of energy ($\Delta_0 = 1$). The dimensionless electron-phonon coupling constant p in the gap equation is determined by Eq. (9) under this condition. The dependence of the superconducting gap Δ on $ev_F A_0$ is weak for $T/T_c \ll 1$ when $ev_F A_0 < \Delta_0$. This is because the shift of energy $|e\mathbf{v}_k \cdot \mathbf{A}_0|$ is small as compared to the range of integration over ϵ in Eq. (9) ($ev_F A_0 \ll \omega_D$; ω_D is the Debye frequency and we put $\omega_D = 8\Delta_0$). The calculations are performed at $T = 0$ because the contribution from the thermally excited quasiparticles to the conductivity is small and $\Delta \simeq \Delta_0$ at low temperatures. The results given below are obtained by the calculation with \mathbf{A}_0 being parallel to $\tilde{E}_\omega^x(q)$ (the perpendicular case corresponds to the term without vertex corrections as mentioned in Sect. 2.1).

When the values of $2\Delta_0/k_B T_c = 3.54$ and $T_c = 1.1$ K are used, the scale of length is numerically given by $1 \mu\text{m} \simeq 0.85 \times 10^{-3}$ as we put $\hbar = c = 1$. However, this scale does not appear explicitly in the numerical calculation, and only dimensionless quantities, $\xi_0 q$ and ξ_0/λ_0 , are needed in calculations ($\xi_0 = v_F/\pi\Delta_0$ is the coherence length). This is because Eq. (4) is rewritten as

$$Z_S = 4\pi i\omega \int \frac{d(\xi_0 q)}{2\pi} \frac{-2\xi_0}{(\xi_0 q)^2 - 4\pi i \xi_0^2 \tilde{j}_\omega^x(q)/\tilde{E}_\omega^x(q)}, \quad (27)$$

and $\tilde{j}_\omega^x(q)$ multiplied by ξ_0^2 is proportional to $(\xi_0/\lambda_0)^2$. [If we take into account a displacement current term in the Maxwell equation Eq. (2), $(\xi_0 q)^2$ is replaced by $(\xi_0 q)^2 - (\xi_0 \omega)^2$. When $\omega \sim 2\Delta_0$ and $\xi_0 \sim 1 \mu\text{m}$, $(\xi_0 \omega)^2 \sim 3.4 \times 10^{-6}$ and then this term can be omitted.]

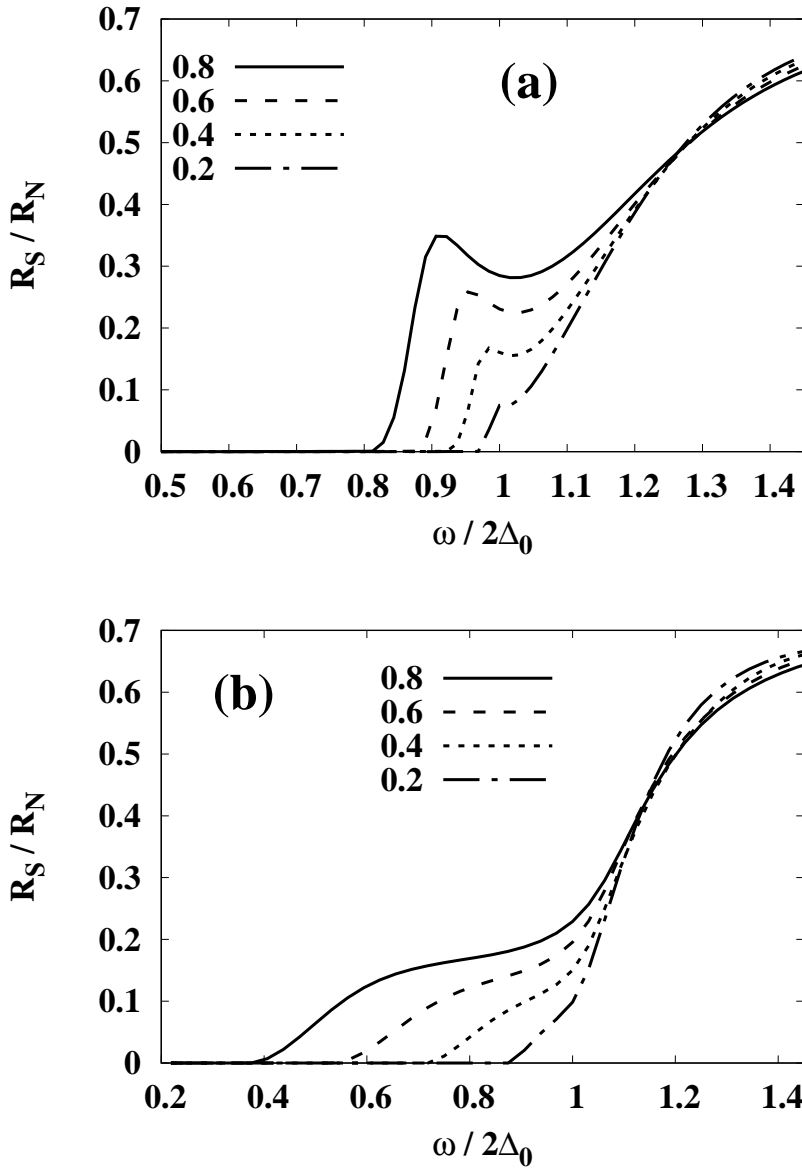


Fig. 1. Dependence of surface resistance on ω for various values of $ev_F A_0$ ($= 0.2, 0.4, 0.6,$ and 0.8). $\xi_0/\lambda_0 = 4.0$. (a) $\alpha = 5.0$ and (b) $\alpha = 0.3$.

3.1 Surface resistance and one-particle spectrum

The calculated surface resistance ($R_S = \text{Re}Z_S$) divided by the quantity in the normal state ($R_N = \text{Re}Z_S|_{\Delta=0}$) is shown Fig. 1. The surface resistance takes finite values below $2\Delta_0$ ($\omega < 2\Delta_0$), and it has a peak in the dirty case ($\alpha = 5.0$). In the relatively clean case ($\alpha = 0.3$), there is a broad tail in R_S for $\omega < 2\Delta_0$. This difference in the spectrum at the gap edge between the dirty and clean cases is related to that in the one-particle spectrum.

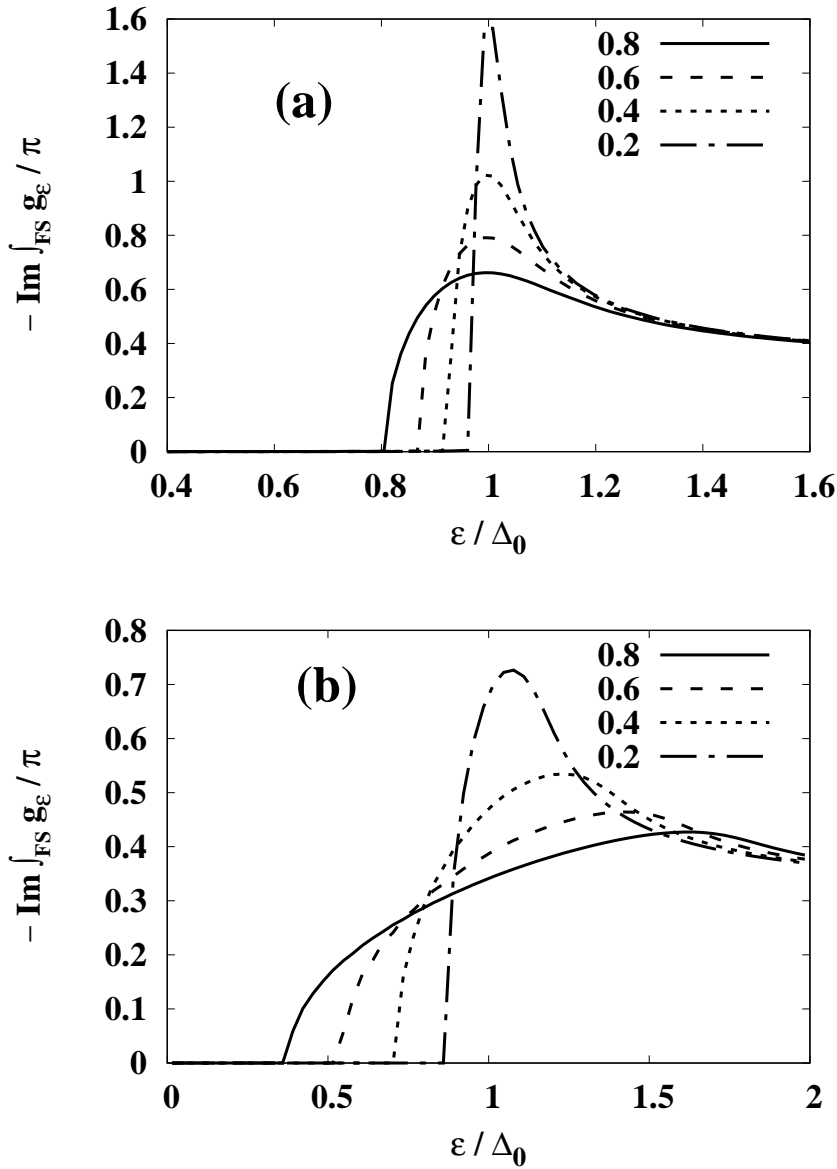


Fig. 2. Density of states for $ev_F A_0 = 0.2, 0.4, 0.6,$ and 0.8 . (a) $\alpha = 5.0$ and (b) $\alpha = 0.3$.

The calculated results of the density of states ($-\text{Im} \int_{\text{FS}} g_{\mathbf{k}, \epsilon}^+ / \pi$) are shown in Fig. 2. In the relatively clean case, the self-energy correction to the one-particle spectrum is small, and the renormalization of the density of states is small. Then, the shift of the spectrum is determined by $ev_{\mathbf{k}} \cdot \mathbf{A}_0$ and the gap edge is close to $\Delta - ev_F A_0$, which is the gap edge in the case with no impurity scattering ($\alpha = 0$). On the other hand, in the dirty case, the impurity scattering renormalizes the shift of the spectrum, and the gap edge shifts to a higher energy, $|\epsilon| \sim E_g = \Delta[1 - (2\alpha_p/\Delta)^{2/3}]^{3/2}$, as in the case with paramagnetic impurities.³³⁾ [α_p is the pair breaking parameter:³⁴⁾ $\alpha_p = (ev_F A_0)^2/6\alpha$.

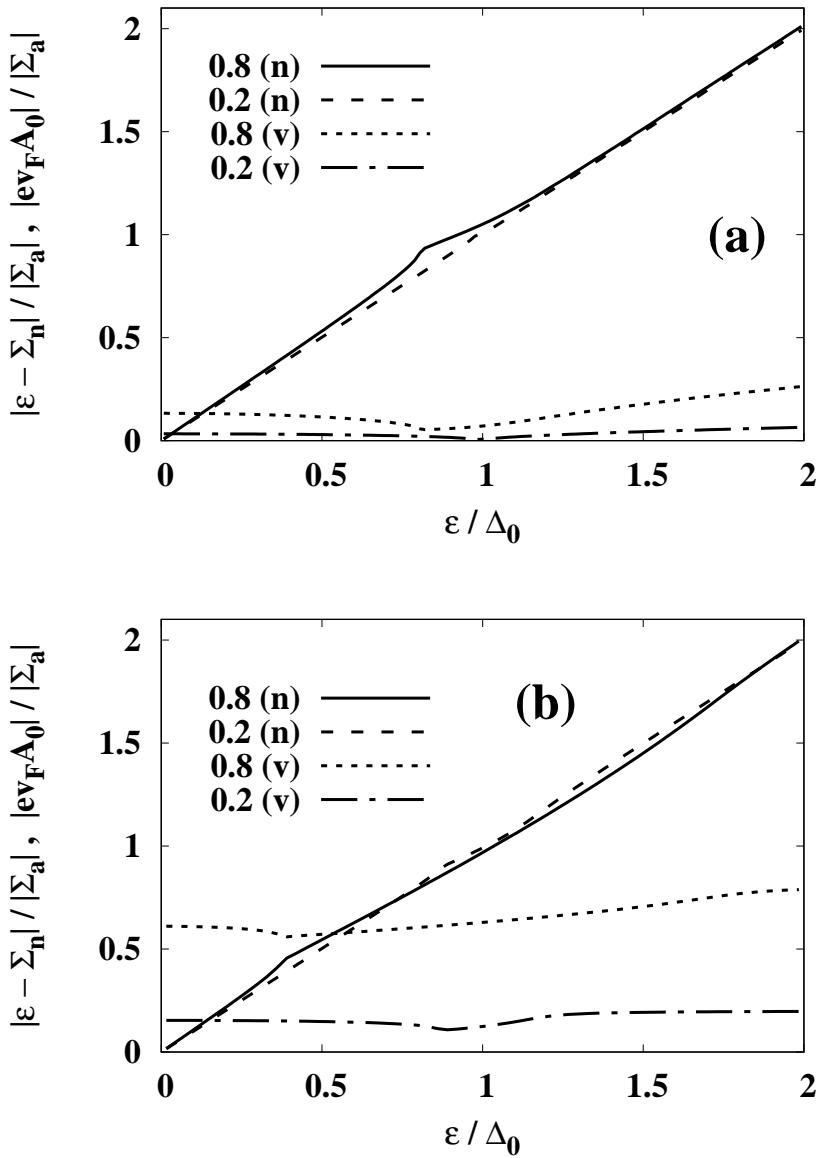


Fig. 3. Dependences of $|\epsilon - \Sigma_n(\epsilon)|/|\Sigma_a(\epsilon)| = (n)$ and $|ev_F A_0|/|\Sigma_a(\epsilon)| = (v)$ on ϵ for $ev_F A_0 = 0.2$ and 0.8 . (a) $\alpha = 5.0$ and (b) $\alpha = 0.3$.

In the case of $ev_F A_0 = 0.8$ and $\Delta = 1$, $E_g \simeq 0.83$ and 0.16 ($\alpha_p \simeq 0.02$ and 0.35) for $\alpha = 5.0$ and 0.3 , respectively. In the clean case ($\alpha < \Delta_0$), this expression is not valid and the gap edge is simply related to the shift ($ev_F A_0$) as noted above.]

The effects mentioned above can be understood by calculating quantities, which include the self-energy corrections, such as $|\epsilon - \Sigma_n(\epsilon)|/|\Sigma_a(\epsilon)|$ and $|ev_F A_0|/|\Sigma_a(\epsilon)|$ [$\Sigma_a^\pm(\epsilon) = \Delta - \alpha \int_{FS} f_{\mathbf{k},\epsilon}^\pm$ given by Eq. (8)] shown in Fig. 3. Equation (13) indicates that the quantities shown in Fig. 3 determine the behavior of the density of states. In

the case of $ev_F A_0 = 0$, $|\epsilon - \Sigma_n(\epsilon)|/|\Sigma_a(\epsilon)| = |\epsilon|/\Delta$ irrespective of the values of α (Anderson's theorem).³⁵⁾ Figure 3 shows that this relation approximately holds for finite values of $ev_F A_0 \neq 0$. On the other hand, the values of $|ev_F A_0|/|\Sigma_a(\epsilon)|$ depend on α and become small for $\alpha > 1$. The renormalization of the density of states results from this dependence of $|ev_F A_0|/|\Sigma_a(\epsilon)|$ on α . (The shift of the gap edge in the density of states has been shown in previous studies.³⁶⁾)

3.2 Vertex correction and spatial variation of conductivity

The physical origin of the peak structure shown in Fig. 1 can be understood by calculating the surface resistance and the conductivity with the use of the decomposition in Eq. (14). The calculated results of several terms for R_S/R_N and $\text{Re}\sigma_q(\omega)/\sigma_0$ ($\sigma_0 = e^2 n_e \tau / m$ with $\tau = 1/2\alpha$) are shown in Fig. 4. These results show that the peak of the surface resistance in the dirty case ($\alpha = 5.0$) originates from the vertex correction by the electron–phonon interaction (amplitude fluctuation). On the other hand, in the clean case ($\alpha = 0.3$), the vertex correction terms are small as compared to the term with no vertex correction, and the contribution of the amplitude mode to the conductivity is relatively small.

The quantity representing the amplitude mode is the denominator of Eq. (20):

$$D_q(\omega) := 1 + p \int \frac{d\epsilon}{2\pi i} \left[T_{\epsilon^-}^h \kappa_{\epsilon^+, \epsilon^-}^{++(v0)}(q) - T_{\epsilon^+}^h \kappa_{\epsilon^+, \epsilon^-}^{--(v0)}(q) + (T_{\epsilon^+}^h - T_{\epsilon^-}^h) \kappa_{\epsilon^+, \epsilon^-}^{+- (v0)}(q) \right]. \quad (28)$$

The real and imaginary parts of $D_{q=0}(\omega)$ are shown in Fig. 5. The results for the real part $\text{Re}D_{q=0}(\omega)$ show that its minimum value around $\omega \simeq 2\Delta$ for the dirty case ($\alpha = 5.0$) is smaller than that for the clean case ($\alpha = 0.3$). The damping $\text{Im}D_{q=0}(\omega)$ shows a different broadness between the clean and dirty cases, which originates from the one-particle density of states as shown in Fig. 2. This behavior of the amplitude mode partly leads to a large (small) electron–phonon vertex correction in the dirty (clean) case as shown in Fig. 4. (This behavior is consistent with the result for the superconductors with paramagnetic impurities shown in Fig. 3 of Ref. 37 because the large (small) values of $ev_F A_0$ (α) correspond to the large values of α_p in Ref. 37.)

From Eqs. (15), (18), (20), and (28), the current including the amplitude mode is rewritten as

$$\tilde{j}_\omega^{x(ep)}(q) = \frac{3p[N_q(\omega)]^2}{2\lambda_0^2 D_q(\omega)} \tilde{A}_\omega^x(q) \quad (29)$$

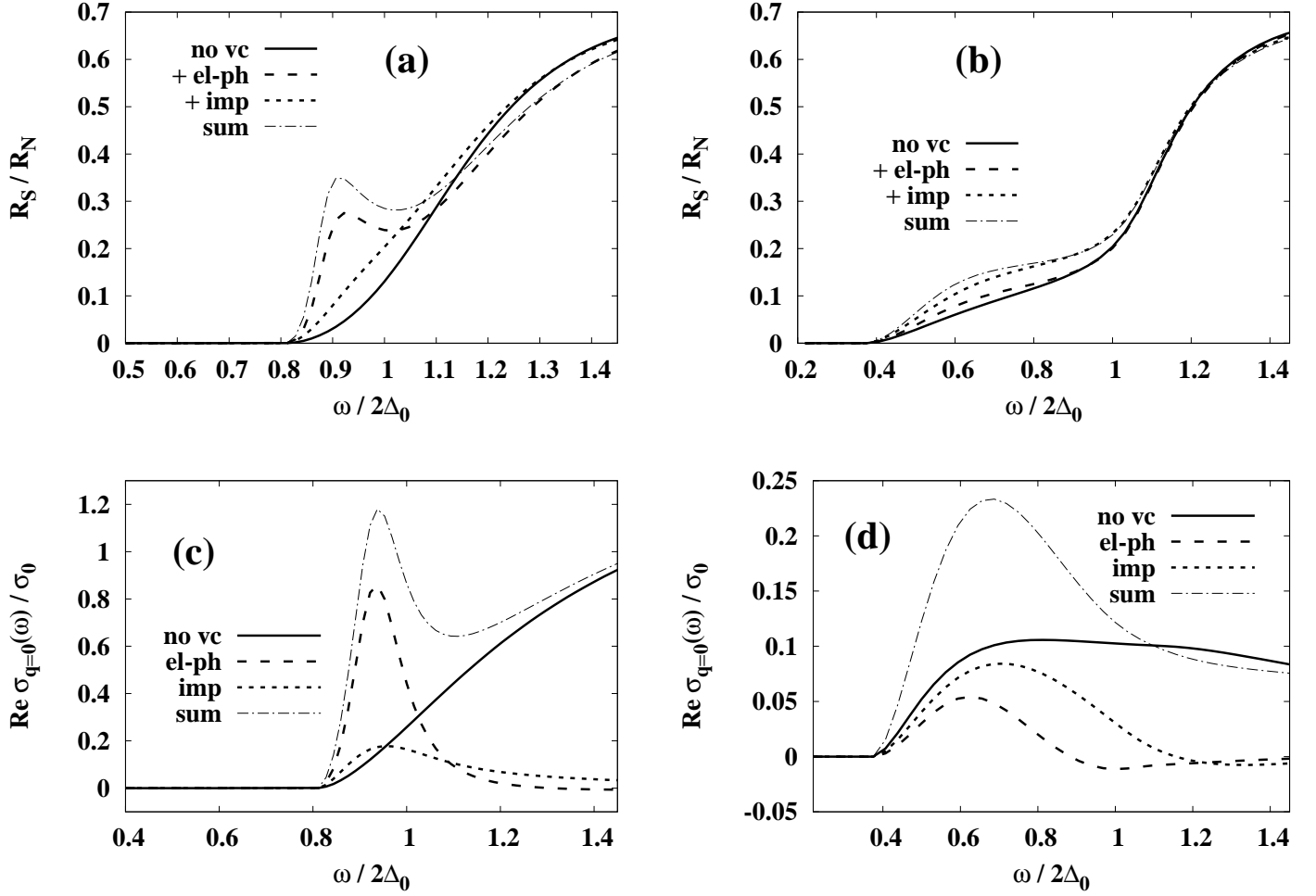


Fig. 4. In (a) and (b), ‘no vc’, ‘+el-ph’, ‘+imp’, and ‘sum’ mean the calculated results with the current $\tilde{j}_\omega^x(q)$ in Eq. (27) replaced by $\tilde{j}_\omega^{x(0)}(q)$, $\tilde{j}_\omega^{x(0)}(q) + \tilde{j}_\omega^{x(ep)}(q)$, $\tilde{j}_\omega^{x(0)}(q) + \tilde{j}_\omega^{x(im)}(q)$, and $\tilde{j}_\omega^x(q)$ (unchanged), respectively. In (c) and (d), ‘no vc’, ‘el-ph’, ‘imp’, and ‘sum’ mean the calculated results of $\text{Re}[\tilde{j}_\omega^{(0)x}(q)/\tilde{E}_\omega^x(q)]_{q=0}/\sigma_0$, $\text{Re}[\tilde{j}_\omega^{x(ep)}(q)/\tilde{E}_\omega^x(q)]_{q=0}/\sigma_0$, $\text{Re}[\tilde{j}_\omega^{x(im)}(q)/\tilde{E}_\omega^x(q)]_{q=0}/\sigma_0$, and $\text{Re}[\tilde{j}_\omega^x(q)/\tilde{E}_\omega^x(q)]_{q=0}/\sigma_0$, respectively. $e v_F A_0 = 0.8$ and $\xi_0/\lambda_0 = 4.0$. $\alpha = 5.0$ for (a) and (c). $\alpha = 0.3$ for (b) and (d).

with

$$N_q(\omega) := \int \frac{d\epsilon}{4\pi i} \left[T_{\epsilon^- \kappa_{\epsilon^+, \epsilon^-}^{++(v1)}}(q) - T_{\epsilon^+ \kappa_{\epsilon^+, \epsilon^-}^{--(v1)}}(q) + (T_{\epsilon^+}^h - T_{\epsilon^-}^h) \kappa_{\epsilon^+, \epsilon^-}^{+-(v1)}(q) \right]. \quad (30)$$

The dependences of $1/|D_{q=0}(\omega)|$ and $|N_{q=0}(\omega)|^2$ on frequency are shown in Fig. 6. There is a peak of $1/|D_{q=0}(\omega)|$ around $\omega \simeq 2\Delta$ in the dirty and clean cases. The peak values in the dirty case are larger than those in the clean case as expected from the results shown in Fig. 5. The term in the numerator of $\tilde{j}_\omega^{x(ep)}(q)$, $N_q(\omega)$, has a large weight around the frequency that corresponds to the gap edge in the one-particle spectrum as

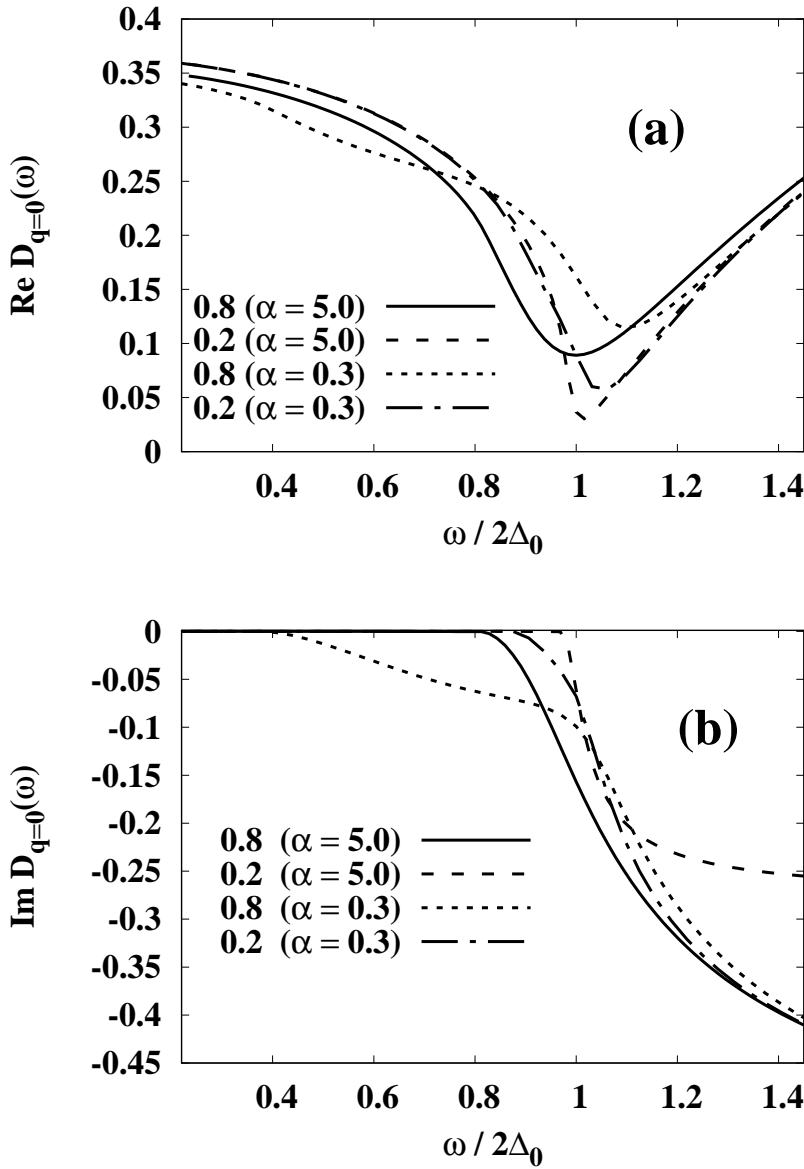


Fig. 5. Dependences of (a) real and (b) imaginary parts of $D_{q=0}(\omega)$ on ω for $ev_F A_0 = 0.2$ and 0.8 . $\alpha = 0.3$ and 5.0 .

in Fig. 2. [This is because the coupling to the external field $ev_{\mathbf{k}}^x \tilde{A}_\omega^x(q)$ is effective in the direction of momentum \mathbf{k} in which there is a large energy shift $|ev_{\mathbf{k}}^x A_0^x|$ ($|v_{\mathbf{k}}^x| \simeq v_F$) in the energy spectrum. The dip around $\omega \simeq 2\Delta$ corresponds to the ineffective coupling to the external field and a small energy shift. On the other hand, in the dirty case, these shifts are averaged out in the energy spectrum owing to the impurity scattering.] Then, in the clean case, there exists a discrepancy between the frequencies at which $1/D_q(\omega)$ and $N_q(\omega)$ take their largest values. This is the reason why the electron–phonon vertex

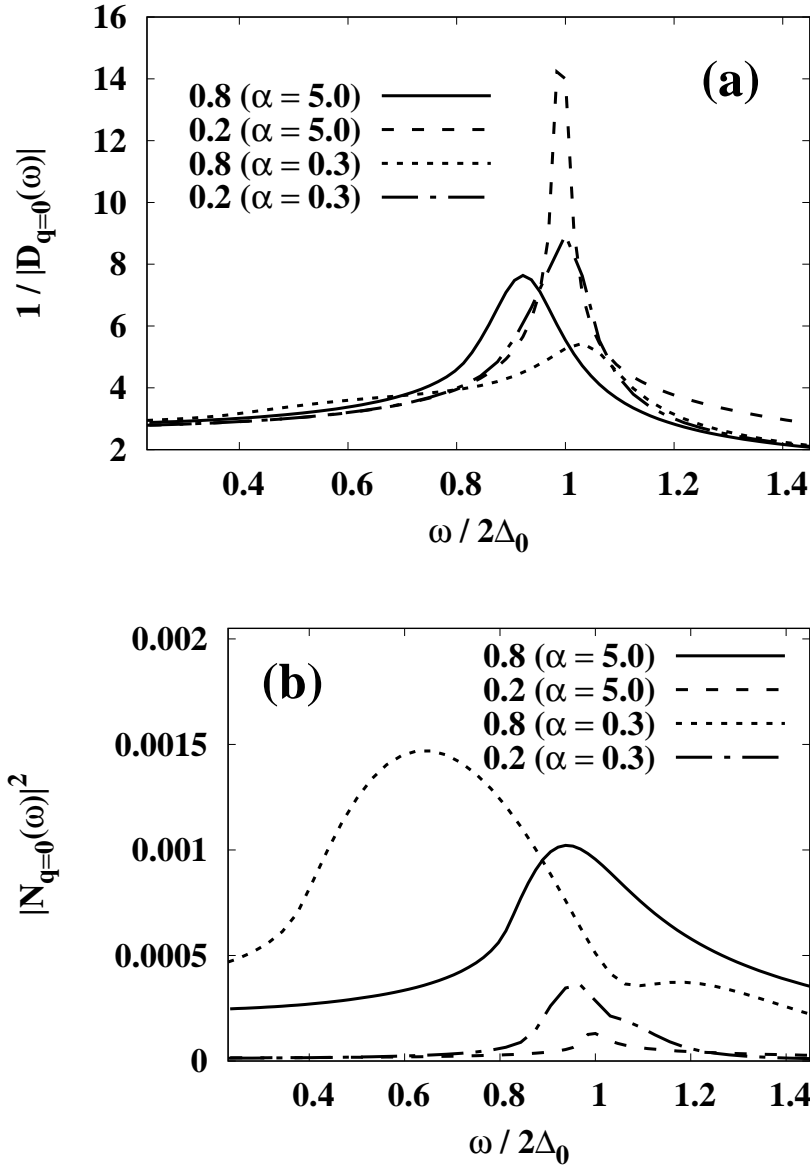


Fig. 6. Dependences of (a) $1/|D_{q=0}(\omega)|$ and (b) $|N_{q=0}(\omega)|^2$ on ω for $ev_F A_0 = 0.2$ and 0.8 . $\alpha = 0.3$ and 5.0 .

correction is not effective for the surface resistance in the clean case as shown in Fig. 4.

The above calculations of R_S are performed in the nonlocal case ($\xi_0/\lambda_0 > 1$), and in this case, the spatial variation (a dependence on q) of conductivity is expected to be important in the calculation of surface impedance. The real part of conductivity for several $\xi_0 q$ values is shown in Fig. 7. Here, $\sigma_q(\omega) = \tilde{j}_\omega^x(q)/\tilde{E}_\omega^x(q)$. $\text{Re}\sigma_q(\omega)/\sigma_0$ does not depend on ξ_0/λ_0 because a factor $1/\lambda_0^2$ in the coefficient of $\tilde{j}_\omega^x(q)$ cancels with that in $\sigma_0 \propto 1/\lambda_0^2$. There is a peak in the absorption spectrum for $q = 0$ even in the relatively

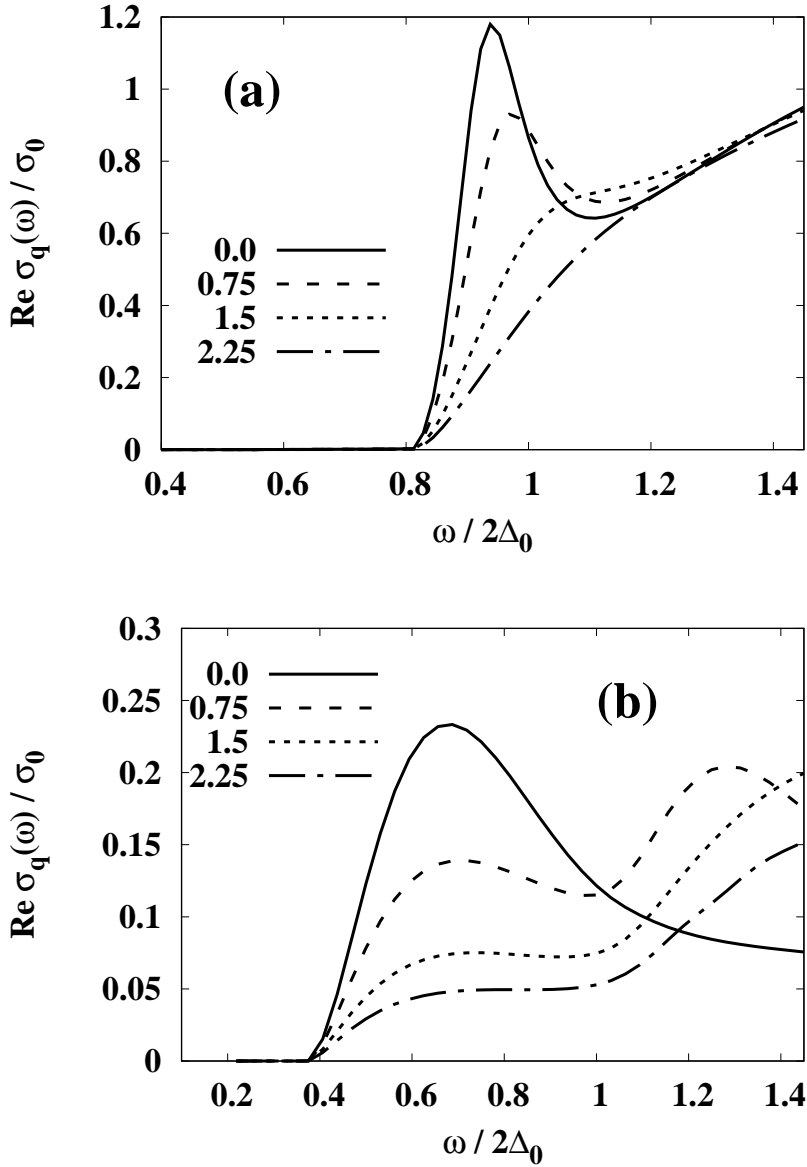


Fig. 7. Dependences of absorptive part of conductivity $\text{Re}\sigma_q(\omega)/\sigma_0$ on ω for various values $\xi_0 q$ ($= 0.0, 0.75, 1.5,$ and 2.25). $ev_F A_0 = 0.8$. (a) $\alpha = 5.0$ and (b) $\alpha = 0.3$

clean case ($\alpha = 0.3$). In the nonlocal case ($\xi_0/\lambda_0 > 1$), however, the surface impedance includes the conductivity over a wide range of wave numbers ($\xi_0 q \sim \xi_0/\lambda_0 > 1$) in the integral [Eq. (27)]. Then, the broad peak in the conductivity is smeared out in the surface resistance in the clean case. On the other hand, in the dirty case, there is a sharp peak in the conductivity because of the amplitude mode and the narrow spectrum in the density of states as in Fig. 2. This results in the peak structure in the surface resistance as shown in Fig. 1.

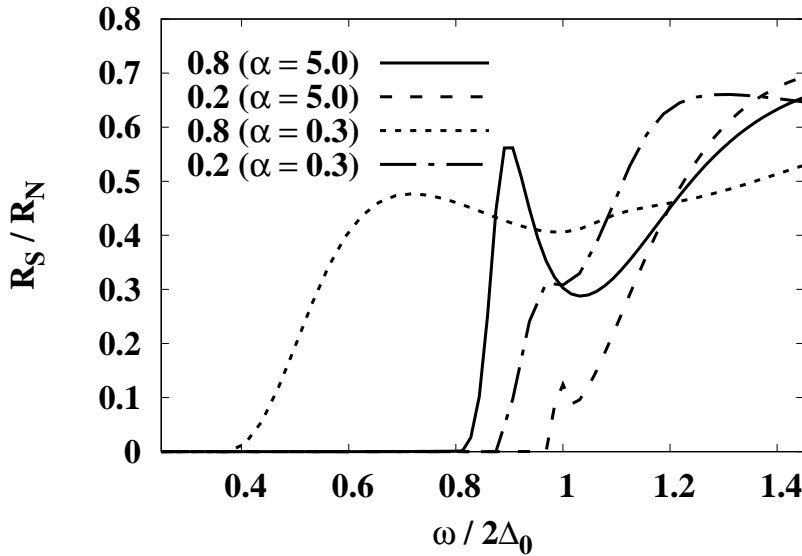


Fig. 8. Surface resistance in local case ($\xi_0/\lambda_0 = 0.25$) with $ev_F A_0 = 0.8$ and $ev_F A_0 = 0.2$ for $\alpha = 5.0$ and $\alpha = 0.3$.

If we consider the local case ($\xi_0/\lambda_0 < 1$), the conductivity at small q ($\xi_0 q \sim \xi_0/\lambda_0 < 1$) mainly contributes to Z_S in the integration of Eq. (27). Then, the peak structure in the surface resistance can be seen even in the clean case. The calculated surface resistance for $\xi_0/\lambda_0 = 0.25$ is shown in Fig. 8. As compared with Fig. 1, the peak structure becomes sharp in the dirty case ($\alpha = 5.0$), and a broad peak can be seen in the clean case ($\alpha = 0.3$). The physical origin of these peaks is different between the dirty and clean cases as shown in Fig. 4. The amplitude mode can be seen in the dirty case, but it is relatively small as compared to other terms in the clean case. The broad peak in the clean case originates from an interlocking between the coupling to the external field and the energy shift as discussed above for $N_q(\omega)$ (Fig. 5).

4. Summary and Discussion

We calculated the surface resistance under a uniform and static external field. Non-locality is taken into account for the dirty and clean superconductors. Although previous studies have concentrated on the local and dirty case, we showed that the peak caused by the amplitude mode appears even in the nonlocal case. The ineffectiveness of the amplitude mode in the clean case is also clarified, and the reason for this is that the weight of the effective coupling to the external field shifts away from that of the amplitude mode.

The calculated results are consistent with the experiment^{23,24)} qualitatively in both dirty and clean cases. (As mentioned below, if the effect of impurity scattering is extremely small, it is possible that other scattering processes, such as electron–phonon interactions, are quantitatively effective for the absorption spectrum.) With use of ξ_0 and the mean free path ($l = v_F\tau$), $\alpha = (\pi\Delta_0/2)(\xi_0/l)$, and the values of $\xi_0/l \sim 7$ and 0.04 for silver-doped Al and pure Al^{23,24)} correspond to $\alpha \simeq 11.0$ and 0.063, respectively. $\xi_0/\lambda_0 > \sqrt{2}$ in both cases. We assumed the static external field to be uniform. If the external field exists in $z < L$, the relation of $ev_F A_0$ to the magnetic field H is written as $ev_F A_0/\Delta_0 = (\pi L/2\sqrt{2}\lambda_0)(H/H_c)$ ($H_c = \hbar c/2\sqrt{2}e\xi_0\lambda_0$). Then, $ev_F A_0/\Delta_0 = 0.8$ corresponds to $H/H_c \simeq 0.72$ in the case of $L = \lambda_0$. This estimation indicates that the uniform A_0 is a first step as an approximation, and the problem with nonuniform A_0 ($\propto e^{-|z|/\lambda_0}$) is a future issue to be solved by calculating the differential equation numerically.

Another issue to be considered is that the dependence of the frequency of the gap edge on the directions of external fields is strong for the clean case in the surface resistance.^{23,24)} In our calculation, there is no difference in the frequency of the gap edge between the surface resistances for $E_x^\omega \parallel \mathbf{A}_0$ and $E_x^\omega \perp \mathbf{A}_0$, which correspond to the term ‘sum’ and ‘no vc’ in Fig. 4(b), respectively. This is because the effect of impurity scattering is integrated over the Fermi surface and the self-energy does not depend on the direction in the momentum space. A possible reason for this discrepancy is the smallness of $\alpha \simeq 0.063$ in experiments. It is possible that the interaction between electrons and acoustic phonons predominates over the impurity scattering effect in the extreme clean case. In this case, the damping rate is written as $\text{Im}\hat{\Sigma}_{\mathbf{k},\epsilon}^{+(ap)} = (p'/4\omega_D^2) \int d\epsilon' (\epsilon - \epsilon') |\epsilon - \epsilon'| (T_{\epsilon'}^h + 1/T_{\epsilon-\epsilon'}^h) \hat{\tau}_3 \text{Im}\hat{g}_{\mathbf{k},\epsilon'}^+ \hat{\tau}_3$ ³⁸⁾ (p' is the contribution to p by acoustic phonons and $p' < 0.56$). This quantity depends on the direction of \mathbf{A}_0 through $e\mathbf{v}_{\mathbf{k}} \cdot \mathbf{A}_0$ and makes the surface resistance dependent on the direction of the external field.

Our calculation indicates that by enhancing the impurity scattering, the frequency of the gap edge will become independent of the relative directions of the external fields (A_x^ω and \mathbf{A}_0). By conducting such an experiment, it will be possible to make a relative comparison between the impurity scattering and the magnitude of electron–acoustic phonon interaction.

Acknowledgment

The numerical computation in this work was carried out at the Yukawa Institute Computer Facility.

References

- 1) C. Giannetti, M. Capone, D. Fausti, M. Fabrizio, F. Parmigiani, and D. Mihailovic, *Adv. Phys.* **65**, 58 (2016).
- 2) M. Beck, M. Klammer, S. Lang, P. Leiderer, V. V. Kabanov, G. N. Gol'tsman, and J. Demsar, *Phys. Rev. Lett.* **107**, 177007 (2011).
- 3) R. Matsunaga, Y. I. Hamada, K. Makise, Y. Uzawa, H. Terai, Z. Wang, and R. Shimano, *Phys. Rev. Lett.* **111**, 057002 (2013).
- 4) R. Matsunaga, N. Tsuji, H. Fujita, A. Sugioka, K. Makise, Y. Uzawa, H. Terai, Z. Wang, H. Aoki, and R. Shimano, *Science* **345**, 1145 (2014).
- 5) K. Katsumi, N. Tsuji, Y. I. Hamada, R. Matsunaga, J. Schneeloch, R. D. Zhong, G. D. Gu, H. Aoki, Y. Gallais, and R. Shimano, *Phys. Rev. Lett.* **120**, 117001 (2018).
- 6) K. Isoyama, N. Yoshikawa, K. Katsumi, J. Wong, N. Shikama, Y. Sakishita, F. Nabeshima, A. Maeda, and R. Shimano, *Commun. Phys.* **4**, 160 (2021).
- 7) R. Grasset, K. Katsumi, P. Massat, H.-H. Wen, X.-H. Chen, Y. Gallais, and R. Shimano, *npj Quantum Mater.* **7**, 4 (2022).
- 8) N. Tsuji, Y. Murakami, and H. Aoki, *Phys. Rev. B* **94**, 224519 (2016).
- 9) T. Jujo, *J. Phys. Soc. Jpn.* **86**, 024709 (2017).
- 10) Y. Murotani and R. Shimano, *Phys. Rev. B* **99**, 224510 (2019).
- 11) M. Shilaev, *Phys. Rev. B* **99**, 224511 (2019).
- 12) L. Schwarz, R. Haenel, and D. Manske, *Phys. Rev. B* **104**, 174508 (2021).
- 13) J. L. Levine, *Phys. Rev.* **155**, 373 (1967).
- 14) A. Anthore, H. Pothier, and D. Esteve, *Phys. Rev. Lett.* **90**, 127001 (2003).
- 15) P. Fulde, *Phys. Rev.* **137**, A783 (1965).
- 16) K. Maki and P. Fulde, *Phys. Rev.* **140**, A1586 (1965).
- 17) T. Jujo, *J. Phys. Soc. Jpn.* **88**, 104701 (2019).
- 18) K. Maki, *Phys. Rev. Lett.* **14**, 98 (1965).
- 19) Yu. N. Ovchinnikov, *Zh. Eksp. Teor. Fiz.* **59**, 128 (1971) [*Sov. Phys. JETP* **32**, 72 (1971)].
- 20) A. Gurevich, *Phys. Rev. Lett.* **113**, 087001 (2014).
- 21) T. Kubo, *Phys. Rev. Appl.* **17**, 014018 (2022).

- 22) A. Moor, A. F. Volkov, and K. B. Efetov, Phys. Rev. Lett. **118**, 047001 (2017).
- 23) W. V. Budzinski and M. P. Garfunkel, Phys. Rev. Lett. **17**, 24 (1966).
- 24) W. V. Budzinski, M. P. Garfunkel, and R. W. Markley, Phys. Rev. B **7**, 1001 (1973).
- 25) P. Pincus, Phys. Rev. **158**, 346 (1967).
- 26) R. D. Sherman, Phys. Rev. B **8**, 173 (1973).
- 27) Yu. N. Ovchinnikov and A. R. Isaakyan, Zh. Eksp. Teor. Fiz. **74**, 178 (1978) [Sov. Phys. JETP **47**, 91 (1978)].
- 28) S. Nakamura, Y. Iida, Y. Murotani, R. Matsunaga, H. Terai, and R. Shimano, Phys. Rev. Lett. **122**, 257001 (2019).
- 29) G. E. H. Reuter and E. H. Sondheimer, Proc. R. Soc. Lond. A **195**, 336 (1948).
- 30) A. A. Abrikosov, *Fundamentals of the Theory of Metals* (North-Holland, Amsterdam, 1988) Chap. 7.
- 31) G. M. Éliashberg, Zh. Eksp. Teor. Fiz. **61**, 1254 (1971) [Sov. Phys. JETP **34**, 668 (1972)].
- 32) Several studies on strong-coupling superconductors^{39,40)} show that there is a peak around $\omega \simeq 2\Delta$ in the real part of the optical conductivity even in the case of $e\mathbf{v}_{\mathbf{k}} \cdot \mathbf{A}_0 = 0$. Then, it is possible that the weak-coupling superconductors, in which the diagonal part of the self-energy by the electron-phonon interaction is negligible, are suitable for the observation of changes in the spectrum around the gap edge with $e\mathbf{v}_{\mathbf{k}} \cdot \mathbf{A}_0 \neq 0$.
- 33) S. Skalski, O. Betbeder-Matibet, and P. R. Weiss, Phys. Rev. **136**, A1500 (1964).
- 34) K. Maki, in *Superconductivity*, ed. R. D. Parks (Dekker, New York, 1969) Chap. 18.
- 35) P. W. Anderson, J. Phys. Chem. Solids **11**, 26 (1959).
- 36) J. Sánchez-Cañizares, J. Ferrer, and F. Sols, Phys. Rev. B **63**, 134504 (2001).
- 37) T. Jujo, J. Phys. Soc. Jpn. **87**, 024704 (2018).
- 38) N. B. Kopnin, *Theory of Nonequilibrium Superconductivity* (Oxford University Press, New York, 2001). Chap. 9, Sect. 9.1.1.
- 39) N. E. Bickers, D. J. Scalapino, R. T. Collins, and Z. Schlesinger, Phys. Rev. B **42**, 67 (1990).
- 40) D. Rainer and J. A. Sauls, in *Superconductivity: From Basic Physics to the Latest Developments*, eds. P. N. Butcher and Y. Lu (World Scientific, Singapore, 1995) p. 45. (arXiv:1809.05264).